



## RESEARCH ARTICLE

### ***In vitro* Infection of Street and Fixed Rabies Virus Strains Inhibit Gene Expression of Actin-Microtubule Binding Proteins EB3 and p140cap in Neurons**

Yidi Guo<sup>1§</sup>, Waqas Ahmad<sup>§1,2</sup>, Ying Song<sup>1§</sup>, Xinyu Wang<sup>1</sup>, Jie Gao<sup>1</sup>, Ming Duan<sup>1</sup>, Zhenhong Guan<sup>1</sup>, Iahtasham Khan<sup>2</sup>, Muhammad Awais<sup>2</sup> and Maolin Zhang\*<sup>1</sup>

<sup>1</sup>Key Laboratory of Zoonosis Research, Ministry of Education, Institute of Zoonosis, College of Veterinary Medicine, Jilin University, 5333 Xian Road, Changchun 130062, People's Republic of China; <sup>2</sup>Section of Epidemiology and Public Health, College of Veterinary and Animal Sciences, Jhang 35200, Pakistan

\*Corresponding author: zhangmaolin@yahoo.com

#### ARTICLE HISTORY (18-293)

Received: August 04, 2018  
Revised: October 22, 2018  
Accepted: November 01, 2018  
Published online: January 24, 2019

#### Key words:

EB3  
Gene expression  
Microtubule  
Neurons  
p140cap  
Rabies virus

#### ABSTRACT

Rabies virus (RABV) is a highly neurotropic pathogen that causes neuronal dysfunction and alters the structural morphology of cytoskeleton. Different factors co-participate in regulating dynamic actin-microtubule cytoskeleton. Although RABV infection has been identified to induce microtubule depolymerization, but the relevant or associated molecular mechanism remains unclear. In order to observe the relation between RABV and cytoskeleton, immunofluorescence was performed to observe the structure of actin-microtubule cytoskeleton and associated binding proteins followed by quantification through experiments of Real-time PCR and western blot. The data showed that RABV disrupted the continuity of microtubules in confocal microscopy, and the localization of EB3 was random and varied at 48 hr and 98 hr of post-infection as compared to mock-infected cells. Street (MRV) and fixed (CVS-11) strains of RABV drastically reduced the gene expression of EB3 protein. These results demonstrated that RABV may alter the neuronal morphology by destructing balance of actin-microtubule cytoskeleton. Moreover, EB3 and p140cap play vital roles in inducing microtubule depolymerization during RABV infection.

©2018 PVJ. All rights reserved

**To Cite This Article:** GuoY, AhmadW, SongY, WangX, GaoJ, DuanM, GuanZ, KhanI, AwaisM and ZhangM, 2019. *In vitro*infection of street and fixed rabies virus strains inhibit gene expression of actin-microtubule binding proteins EB3 and p140cap in Neurons. Pak Vet J. <http://dx.doi.org/10.29261/pakvetj/2019.007>

#### INTRODUCTION

Rabies virus (RABV) as a member of the *Lyssavirus* genus of the *Rhabdoviridae* family is the cause of horrifying neurological disease leading to agonizing death. RABV manifests strong affinity for the nervous system by binding specific neural receptors (Sasaki *et al.*, 2018; Wang *et al.*, 2018) and propagates its own trafficking (Gluska *et al.*, 2014), replication (Zhanget *et al.*, 2017) and budding (Zan *et al.*, 2016) in nerve cells. RABV encodes five viral proteins: nucleoprotein (N), phosphoprotein (P), matrix protein (M), glycoprotein (G), and the large protein (also termed RNA-dependent RNA polymerase, RdRp, L). The ribonucleoprotein (RNP) complex is formed by the viral RNA genome and the capsidating N protein, P protein, M protein, facilitating viral entry, replication, budding and releasing, respectively (Zhang *et al.*, 2017).

The abnormality of neurological function is considered a principal neurological symptom of rabies (Scott *et al.*, 2008) and might be associated with the neuronal cytoskeleton which maintains cellular morphology, fiber network and regulates intracellular movement related functions (Kapitein and Casper, 2015). Neuronal cytoskeleton comprises of actin, microtubule and intermediate filaments. The microtubule is a polarized elongated heterodimer of  $\alpha$  and  $\beta$  tubulin subunits, and play crucial roles in cellular & biological processes, such as mitotic cell division, endosomal signaling and molecular cargoes trafficking (Zan *et al.*, 2016). Microtubule abnormality is closely associated with neuronal dysfunction (Chen *et al.*, 2012) which implicates that RABV infection may change or modify the microtubule dynamics. The structural and biochemical profile of microtubules are regulated by post-translational modifications (Wloga *et al.*, 2017) and microtubule-associated proteins (Alfaro-Aco and Petry, 2015). Microtubules maintain neuronal growth and shape

<sup>§</sup>These authors contributed equally to this work.

through highly differentiated cellular polarity due to their mixed arrangements of elongated filaments in the long ranged axons (Rasband, 2010). The plus ends of the microtubule filament are usually directed towards the cell periphery and undergo continuous polymerization and depolymerization respectively (Kleele *et al.*, 2014).

Among microtubule plus-end tracking proteins (+TIPS) distinguished by their specific accumulation at microtubule plus ends, the end binding (EB) family proteins physically interrelate with rest of +TIPs to recruit them to microtubule ends and involves in microtubule-associated signaling pathways (Rasband, 2010). Three known proteins of EB (EB1, EB2 and EB3) are found, and among these EB3, as a kind of relatively conservative dimeric protein belonging to the third family member of RP/EB group, is involved in the regulation of microtubule dynamics in central nervous system (Nakagawa *et al.*, 2000). It consists of 281 amino acid residues, containing an N-terminal structure of calmodulin homologous sites, and a C-terminal coiled-coil domain used to form a dimer that can interact with p140cap and APCL (Nakagawa *et al.*, 2000; Komarova *et al.*, 2009). In addition, microtubules also interact with the filamentous actin to bring about these transport and polarity functions (Kapitein and Casper, 2015). According to parallel studies, TIPs are important for crosstalk between dynamic actin and microtubule cytoskeleton (Alfaro-Aco and Petry, 2015) and EB3 may be the key regulator (Jaworski *et al.*, 2009). The p140cap is also known as SNIP; SNAP-25 interacting protein (Chin *et al.*, 2000), and inhibits Src kinase activity to regulate dynamic actin cytoskeleton together, as a Src-binding protein, interacts with EB3 and plays vital role in postsynaptic density, dendritic spine functions and morphology (Jaworski *et al.*, 2009).

Previous studies have shown that the fixed challenge virus strain (CVS-11) and street strain (MRV) of RABV cause severe pathological changes in neuronal cytoskeleton (Zan *et al.*, 2017). Since both dynamic actin and microtubule are disrupted under infection of RABV, some key regulators may play crucial roles. In the present study, CVS-11 strain was used to screen mRNA expression of different microtubule and actin associated proteins, then experiments were focused on EB3 and its binding partner p140cap. Through investigating the transcription, expression, distribution of EB3 and p140cap in neurons infected with CVS-11 and MRV, it would be helpful to further understand the mechanism of RABV destructing dynamic cytoskeleton.

## MATERIALS AND METHODS

**Animals and strains:** Pregnant female rats were purchased from Changchun Animal Center and acclimatized before the start of experiments. All the procedures regarding animal handling and care were carried out in accordance with the Institutional Animal Welfare Act of Jilin University. The CVS-11 and MRV of RABV were kindly given to us by the Changchun Veterinary Research Institute, OIE Rabies Reference Laboratory of Changchun.

**Cell culture and virus inoculation:** The primary cortical neuron cultures were prepared from embryonic day 16.5

mice embryos. After suspended adequately with Dulbecco's modified Eagle's medium (DMEM; Invitrogen), the cortices were digested by 0.25% trypsin (Invitrogen) with 50  $\mu$ l of 10 mg/ml DNase I stock (Invitrogen) added for 10 min at 37°C. The cells were then titrated in glass pipettes as soon as digestion terminated. The cell suspension was adjusted to the appropriate concentration, then initially plated with 10% FBS/DMEM in 37°C, 5% CO<sub>2</sub> incubator. After 4 hrs, the medium was carefully replaced with neurobasal medium (Invitrogen) supplemented with B27 (Gibco) and 2 mM L-glutamine (Invitrogen). The cells grew for up to 10 days without any further change of medium. The cells were infected with MRV and CVS-11 at 10 TCID<sub>50</sub> per well and subsequently cultured in neurobasal medium.

**RNA preparation and Real Time PCR:** Total RNA was isolated using Trizol, and reverse transcription was performed according to the manufacturer's instructions (PrimeScript RT reagent Kit with gDNA Eraser, Takara). SYBR Green quantitative polymerase chain reaction (PCR) kit was purchased from Roche (Catalogue No. 4913914001). The set of RT-PCR primer sequences are listed below:

EB3-F GTGGACAAAATCATTCCCGTA, EB3-RTTTC CATCATAGTTTGGCGTCA; p140cap-F ATAAAGGCA AACACGGCAAG, p140capR TTAAGACAGCGGCAT ATAGCA; Tppp-F CGGATACCAGCAAGTTCACAG, Tppp-R ACGTAGCCTGACTCATCCAC; Ena-F TTCA AAGTCCGATGCCAACC, Ena-R AGGATCTTCCGTT TGGTTCTCA; Vasp-F TCCCTGCCCAAAGTGAACC TG, Vasp-R TCTGTAGCTCCTTCCGCACCT; Fascin1-FTACAACATCAAAGACTCCACGG, Fascin1-R GAG AGCCACCTTATTGTAGTCAC.

**Western blot:** Whole cell extracts were prepared by RIPA lysis buffer (pp1901, Biotek), which contains a protease inhibitor mixture (Roche Applied Science). The protein concentrations of whole cell lysates were determined by BCA kit (23227, Thermo). Equal amounts of protein were boiled with SDS sample buffer (WB2001, NCM) for 5 minutes, fractionated by 10% SDS polyacrylamide gels (PAGE) and transferred to polyvinylidene fluoride (PVDF) membranes. After blocking in TBST with 3% bovine serum albumin (BSA) at 37°C for 1 hr, the membranes were incubated with primary antibodies against EB3 (ab157217, Abcam),  $\beta$ -actin (#3700S, Cell signaling technology), p140cap (#3757, Cell signaling technology) at 4°C overnight, washed 4 $\times$ 15 minutes in TBST, and incubated with appropriate horseradish peroxidase (HRP)-conjugated goat anti-rabbit polyclonal antibody (bs-0295G, Bioss, USA) or HRP-conjugated goat anti-mouse monoclonal antibody (bs-0296G, Bioss, USA) at 37°C for 1 hr. The membranes were washed 4 $\times$ 15 minutes in TBST and visualized by MicroChem 4.2.

**Immunofluorescence:** At the indicated hours post-infection, the cortical neuronal cells were fixed with 4% paraformaldehyde in 0.1 M phosphate buffer containing 0.1% Triton X-100 for 30 min at room temperature. The cultured cells on glass slides were incubated with primary antibodies overnight at 4°C right after blocking. After

washing with 0.1 M phosphate buffer saline, the Alexa Fluor® 594-conjugated goat anti-Rabbit IgG (1:100, A-11072, Invitrogen) was applied. Cellular nuclei were stained with Hoechst (33258, Sigma). Cy3-conjugated anti- $\beta$ -tubulin-antibody (ab11309, Abcam), FITC Anti-Rabies Monoclonal Globulin (# 800-092, FUJIREBIO) were also utilized. Fluorescence photography was captured with a confocal microscope (Olympus).

**Statistical analyses:** All of the data were presented as mean $\pm$ SD and analyzed by SPSS statistical software. The western blot results were procured through Image J software. Statistical analysis was conducted using Student's t test or one-way ANOVA with Graph Pad Prism 5 software. A probability value with  $P < 0.05$  was considered statistically significant.

## RESULTS

**RABV Disrupts Neuronal Microtubules:** To examine the effect of RABV on microtubules, the cultured neuronal cells were infected with CVS-11 at 10 TCID<sub>50</sub> in vitro day 10 (DIV10), and immunofluorescence analysis with anti- $\beta$ -tubulin and Hoechst was performed (Fig. 1). At 96 h post-infection, disrupted orientation of filamentous microtubules along the entire long-ranged length of axons, and even around the periphery of nucleus (Fig. 1A upper image set), while smooth and refine structure of filamentous neuronal microtubules running in continuity along the projected length of axons showed in mock-infected cells (Fig. 1A lower image set). This suggests that CVS-11 causes fracture of filamentous microtubules and may further reduce the structural stability of axons in neuron cells.

**CVS-11 and MRV Down-regulate Gene Expression of EB3 and p140cap:** Since we found that CVS-11 infection disintegrated elongated microtubule fragments

(Fig. 1), we next wanted to figure out key regulators involved in dynamic microtubule cytoskeleton after CVS-11 infection. For this purpose, proteins were screened for transcription analyses by Real-time PCR assay in CVS-11 infection neurons, and molecules whose transcription level varied obviously were shown in Fig. 2A. The data showed that after 48 hrs of CVS-11 infection, the transcription of microtubule associated proteins, such as EB3 and Tppp, were considerably decreased compared with the control group, and CVS-11 infection also reduced RNA level of several actin binding proteins, like p140cap, Fascin1, Vasp, Ena. Interestingly, EB3 and p140cap, which of both interacts directly and may play crucial roles in overlaps of microtubule and actin, were both repressed.

To further investigate the mechanism of disintegrated filamentous microtubule and clarify how RABV regulates gene expression of EB3 and p140cap, both CVS-11 and MRV strains were used to infect neurons. The results revealed that the transcription level of EB3 reduced even at different time intervals (6 hrs, 12 hrs, 24 hrs, 48 hrs) of CVS-11 infection at 10 DIV ( $X \pm SD$ ,  $P < 0.05$  for  $n = 5$ ) (Fig. 2b). The transcription of EB3 sharply declined until 24 hrs post-infection and maintained reduction as compared with mock-infected control. However, the reduction level rebounded again at 48 hrs of post-infection. Meanwhile, transcription level of p140cap decreased consistently, lower than the control group. The gap between CVS-11 infected cells and mock-infected cells was greatest at 12 hrs post-infection but almost vanished at 48 hrs post-infection (Fig. 2c). In case of MRV, the RNA levels of EB3 (Fig. 2d) decreased from 0 to 6 hrs, 12 hrs, 24 hrs and 48 hrs of post-infection as compared with the control group ( $X \pm SD$ ,  $P < 0.05$  for  $n = 5$ ) without rebound. The variation of p140cap transcription was similar to cells infected with CVS-11, but differences between MRV-infected groups and mock was more moderate (Fig. 2e).

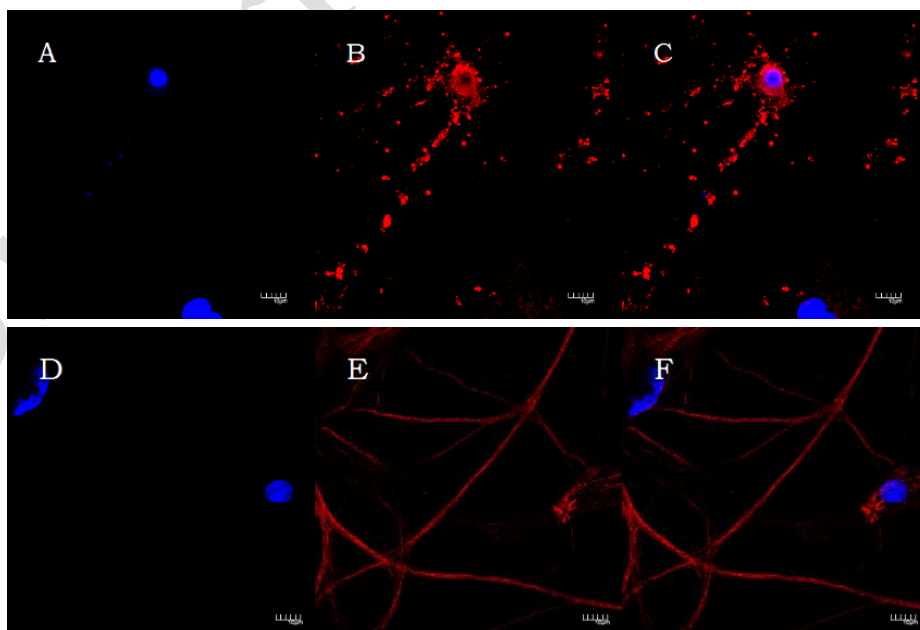


**Fig. 1:** CVS-11 infection disrupts microtubule cytoskeleton. Cortical neurons were infected by CVS-11 at 96 hrs (upper image set), while control cells were mock-infected (lower image set). The cells were fixed, permeabilized and incubated with Alexa 594-conjugated monoclonal antibody tubulins (red), while nuclei were stained with Hoechst (blue).

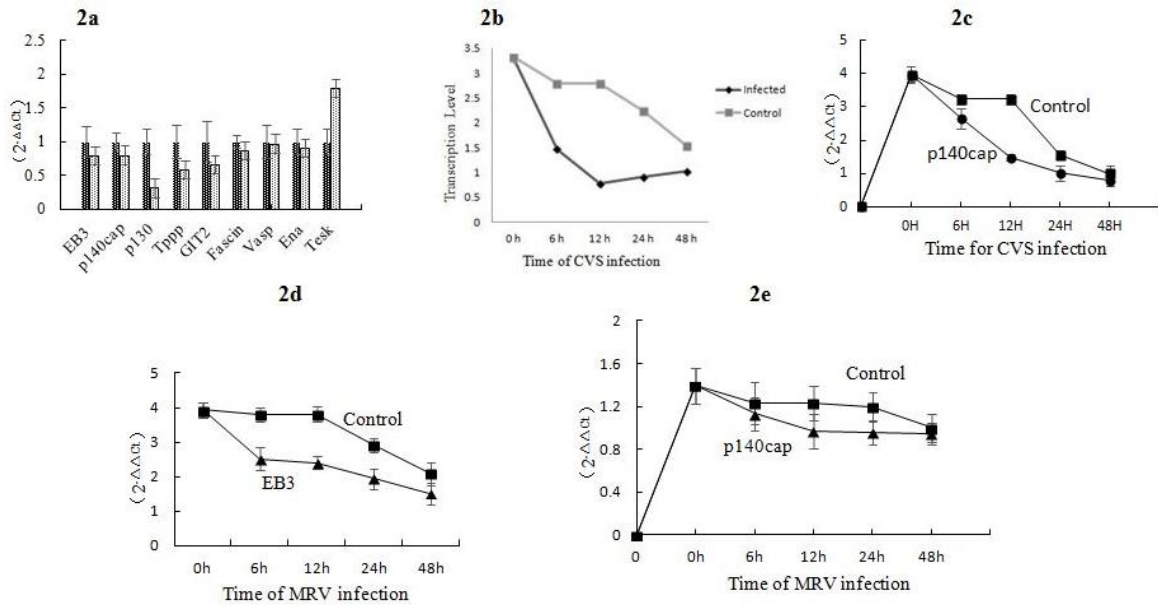


**Fig. 2:** Effects of RABV infection on EB3 and p140cap transcription (2A) Cortical neurons were infected by 48 h at 10 DIV, mRNA level of EB3, p140cap, Tppp, FascinI, Vasp, Ena were analyzed compared with mock-infected cells by Real-time PCR assay. (2B & 2C) The mRNA level of EB3 (2B) and p140cap (2C) at different time intervals (6, 12, 24, 48 h) (2D and 2E). The mRNA level of EB3 (D) and p140cap (E) at different time intervals (6, 12, 24, 48 h) of MRV infection at 10 DIV. The data are presented as the means $\pm$ SD (n=5; \*represents P<0.05, \*\*represents P<0.01).

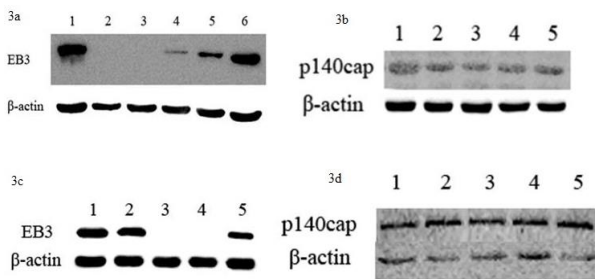


**Fig. 3:** Effects of RABV infection on EB3 and p140cap expression using western blots (3A) The first and last column of the fig. corresponds to the mock-infected cells at 48 h and 1 h time intervals, while 2, 3, 4 and 5 corresponds to 48 hrs, 12hrs, 6hrs and 1 hr of CVS-11 post-infection respectively.(3B) The first and last column of the fig. corresponds to the mock-infected cells at 48 h and 1 h time intervals, while column 2, 3, 4 correspond to 48hrs, 12 hrs and 6 hrs of CVS-11 post-infection respectively.(3C) Column 1 and 2 correspond to the mock-infected cells at 48 hrs and 12 hrs, while column 3, 4, 5 correspond to 48 hrs, 12 hrs, 6 hrs of MRV post-infection.(3D)Column 1, 2 correspond to the mock-infected cells at 48 hrs and 12 hrs, while column 3, 4 and 5 correspond to 48 hrs, 12 hrs, 6 hrs of MRV post-infection.

### CVS-11 Reduces Protein Amounts of EB3 and p140cap:

To clarify CVS-11 and MRV expression of EB3 and p140cap, western blot was performed with extracts from neurons. In Fig. 3a, the first and last column of the figure corresponds to the mock-infected cells at 48 hrs and 1 hr time intervals, while 2, 3, 4 and 5 corresponds to 48 hrs 12 hrs, 6 hrs and 1 h of CVS-11 post-infection respectively (X $\pm$ SD, P<0.05 for n=5). The expression of EB3 significantly reduced at 1 hr post-infection and kept on reducing with the extension of infection time. At 12 hrs and 48 hrs of post-infection, the bands were almost invisible. Meantime, protein level of p140cap decreased slightly at 6 hrs, 12 hrs, 48 hrs post-infection (column 4, 3, 2) compared to those in mock-infected cells (column 5: 1h; column 1:48hrs) (Fig. 3b). During MRV infection, the protein amounts of EB3 significantly decreased from 6 hrs of post-infection (column 5) until vanished at 12 hrs and 48 hrs as shown in column 4 and 3 (Fig. 3c). On the other

hand, MRV did not result in any significant reduction of expression of p140cap at these time intervals (Fig. 3d). Collectively these findings suggest that RABV regulates the gene expression of EB3 and p140cap in neuronal cells.

**Effect of CVS-11 on EB3 in Neuronal Cells:** To further study the role of RABV in regulating EB3, the neuronal cells were stained with anti-EB3 right after FITC Anti-Rabies Monoclonal Globulin at 48 hrs post-infection. As observed in Fig. 4, EB3 localized discontinuously in axons and dendrites, and appeared in the form of thick fluorescent dots along the entire lengths of axons and the cell body. At some axonal branches, pauses of degenerated microtubules were also observed. The EB3 was also unevenly distributed in the cytoplasm and scattered near the cell membrane. At 96 hrs of post-infection, the neurons grew with sprawling axonal branches and dendrites. The localization of EB3 remained unevenly distributed around the cell bodies and along the axonal projections and revealed more abundant thick fluorescent spots measured to be 2  $\mu$ m in diameter. The granular inclusion bodies of RABV were concentrated inside the cell body at 48 hrs of infection, but this was not more apparent in 96 hrs of infection. Instead, the multiple size of green fluorescent viral particles was scattered inside the cell body (Fig. 4I-P).

## DISCUSSION

Microtubules contribute to neuronal morphology (Van de Willige *et al.*, 2016) and dynamic intracellular events, such as cellular division, signaling and intracellular trafficking (López-Doménech *et al.*, 2018) in coordination with the actin cytoskeleton (Colin *et al.*, 2018). Few other viruses also rely on microtubules to achieve intracellular trafficking, including HIV-1 (Dharan and Campbell, 2018), vaccinia virus (Leite *et al.*, 2015), herpes virus (Paseloup *et al.*, 2013) and Circovirus (Cao

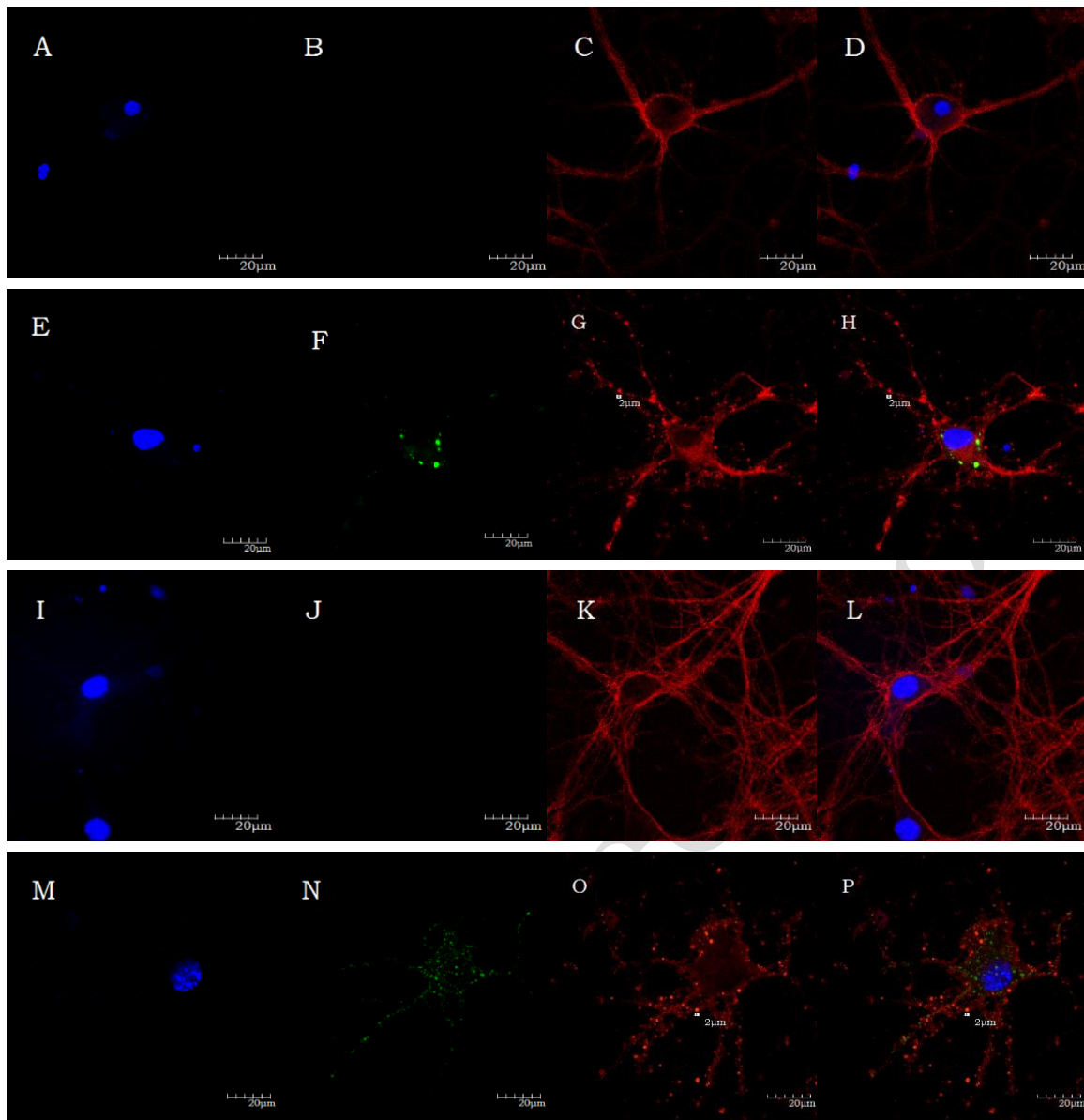


**Fig. 4:** Effects of CVS-11 infection on localization of EB3. Representative images of cortical neurons were double labeled with anti-RABV antibody (green) and anti-EB3 antibody (red) at 48 h in control (A–D) and CVS-11 infected cells (E–H), while (I–L) and (M–P) show control and experimental neurons at 96 h post-infection, respectively.

*et al.*, 2015). Currently,  $\alpha$ -tubulin was reported to be incorporated into RABV particles, which suggests that the microtubule might play a role in RABV infection as RABV disrupts cytoskeleton dynamics.

Microtubule dynamics is mainly affected by multiple factors, and EB family protein is among these factors that belong to the +TIPs (Akhmanova and Steinmetz, 2015; Zhang *et al.*, 2015). Among EB family proteins, EB3 is a kind of relatively conservative dimeric protein accumulated at growing microtubule plus ends, which is involved in the microtubule dynamics regulation in central nervous system (Nakagawa *et al.*, 2000; Yang *et al.*, 2017). The p140cap is a binding partner of EB3 that also maintains the assembly of actin by binding with Src kinase (Jaworski *et al.*, 2009). Src phosphorylation involves in signaling-pathway like WASP [Wiskott-Aldrich syndrome protein]-Arp2/3 regulating actin assembly and branching (Colin *et al.*, 2018). The p140cap is controlled by the action of semaphoring signaling pathways that maintain the actin dynamics (López-

Doménech *et al.*, 2018). Besides microtubules-actin coordination, interaction between these two cytoskeletal domains affects neuritis morphology in some ways (Fukushima and Morita, 2006). EB3 regulate the localization of p140cap modulate actin dynamics within dendritic spines (Jaworski *et al.*, 2009), implying that EB3 and p140cap may be a novel link between microtubules and actin cytoskeleton. In this study, the transcription and expression levels of EB3 and p140cap showed a decline in different degrees after CVS-11 and MRV infection (Fig. 2 and 3). Localization of EB3 distributed randomly along neuronal axons and represented abundant thick dots at 48 hrs post-infection, which phenomenon became more apparent (Fig. 4). These results showed a relationship between EB3 linked plus ends of microtubule and p140cap in agreement with previous findings. This kind of association also governs the signaling events of actin and microtubules in the dendritic spines (Jaworski *et al.*, 2009). As p140cap was associated with actin polymerization and regulated by EB3, more work about

effects of RABV on p140cap related to signaling pathway and stability of actin cytoskeleton should be extended.

The RT-qPCR screening results showed the down-regulation of EB3, p140cap, Fascin1, Tppp, Vasp, and Ena mRNAs (Fig. 2A). However, the reduction was moderate compared to p130 which has more than 50% decrease of mRNA. Moreover, there was an increase of Tesk mRNA. Taking these results into consideration, it is possible that the infection of RABV may cause the neurons to undergo apoptosis and the microtubule is depolymerized in apoptotic cells (Akhmanova and Steinmetz, 2015).

Collectively, our study reveals for the first time, that EB3 and p140cap were regulated by infection of CVS-11 and MRV and involved in inducing microtubule depolymerization. Although it remains unknown for us how RABV regulates gene expression of EB3 and p140cap in details as well as relevant signaling pathways, the finding that these two cofactors are involved in RABV impairing microtubule polymerization is important.

**Acknowledgments:** This study was supported by the Grants No. 216YFD0500402 from National Key Research and Development Program of China, and Grants No. 31472208 and 31272579 from Natural Science Foundation of China. We also acknowledge the kind support made by Federal German Foreign Office research project title "Development of Lab networking under biosafety and biosecurity aspects in Pakistan" for the accomplishment of this research work.

**Authors contribution:** YG, WA and YS performed immunofluorescence and cell culture. XW, JG and MD conceived and designed the study plan, and performed real time PCR. ZG and MZ performed western blots. IK and MA wrote manuscript, analyzed data and critically revised the manuscript. All authors interpreted the data, read the manuscript for important intellectual contents and approved the final version.

## REFERENCES

- Akhmanova A and Steinmetz MO, 2015. Control of microtubule organization and dynamics: two ends in the limelight. *Nat Rev Mol Cell Biol* 16:711-26.
- Alfaro-Aco R and Petry S, 2015. Building the Microtubule Cytoskeleton Piece by Piece. *J Biol Chem* 290:17154-62.
- Cao J, Lin C, Wang H, et al., 2015. Circovirus transport proceeds via direct interaction of the cytoplasmic dynein ICI subunit with the viral capsid protein. *J Virol* 89:2777-91.
- Chen L, Stone MC, Tao J, et al., 2012. Axon injury and stress trigger a microtubule-based neuroprotective pathway. *Proc Natl Acad Sci USA* 109:11842-7.
- Chin LS, Nugent RD, Raynor MC, et al., 2000. SNIP, a novel SNAP-25-interacting protein implicated in regulated exocytosis. *J Biol Chem* 275:1191-200.
- Colin A, Singaravelu P, Théry M, et al., 2018. Actin-Network Architecture Regulates Microtubule Dynamics. *Curr Biol* 28:2647-56.
- Dharan A, Campbell EM, 2018. Role of Microtubules and Microtubule-Associated Proteins in HIV-1 Infection. *J Virol* 92:e1004348.
- Fukushima N and Morita Y, 2006. Actomyosin-dependent microtubule rearrangement in lysophosphatidic acid-induced neurite remodeling of young cortical neurons. *Brain Res* 1094:65-75.
- Gluska S, Zahavi EE, Chein M, et al., 2014. Rabies Virus Hijacks and accelerates the p75NTR retrograde axonal transport machinery. *PLoS Pathog* 10:e1004348.
- Jaworski J, Kapitein LC, Gouveia SM, et al., 2009. Dynamic microtubules regulate dendritic spine morphology and synaptic plasticity. *Neuron* 61:85-100.
- Kapitein LC and Casper CH, 2015. Building the Neuronal Microtubule Cytoskeleton. *Neuron* 87:492-506.
- Kleele T, Marinkovic P, Williams PR, et al., 2014. An assay to image neuronal microtubule dynamics in mice. *Nat Commun* 5:4827-9.
- Komarova Y, De Groot CO, Grigoriev I, et al., 2009. Mammalian end binding proteins control persistent microtubule growth. *J Cell Biol* 184:691-706.
- Leite F and Way M, 2015. The role of signaling and the cytoskeleton during Vaccinia Virus egress. *Virus Res* 209:87-99.
- López-Doménech G, Covill-Cooke C, Ivankovic D, et al., 2018. Miro proteins coordinate microtubule- and actin-dependent mitochondrial transport and distribution. *EMBO J* 37:321-36.
- Nakagawa H, Koyama K, Murata Y, et al., 2000. EB3, a novel member of the EBI family preferentially expressed in the central nervous system, binds to a CNS-specific APC homologue. *Oncog* 13:1-6.
- Pasdeloup D, McElwee M, Beilstein F, et al., 2013. Herpesvirus tegument protein pUL37 interacts with dystonin/BPAG1 to promote capsid transport on microtubules during egress. *J Virol* 87:2857-67.
- Rasband MN, 2010. The axon initial segment and the maintenance of neuronal polarity. *Nat Rev Neurosci* 11:552-62.
- Sasaki M, Anindita PD, Ito N, et al., 2018. Heparan sulfate proteoglycans serve as an attachment factor for rabies virus entry and infection. *J Infect Dis* 217:1740-9.
- Scott CA, Rossiter JP, Andrew RD, et al., 2008. Structural abnormalities in neurons are sufficient to explain the clinical disease and fatal outcome of experimental rabies in yellow fluorescent protein-expressing transgenic mice. *J Virol* 82:513-21.
- Van de Willige, Hoogenraad CC and Akhmanova A, 2016. Microtubule plus-end tracking proteins in neuronal development. *Cell Mol Life Sci* 73:2053-77.
- Wang J, Wang Z, Liu R, et al., 2018. Metabotropic glutamate receptor subtype 2 is a cellular receptor for rabies virus. *PLoS Pathog* 14:e1007189.
- Wloga D, Joachimiak E and Fabczak H, 2017. Tubulin Post-Translational Modifications and Microtubule Dynamics. *Int J Mol Sci* 18:2207.
- Yang C, Wu J, de Heus C, et al., 2017. EBI and EB3 regulate microtubule minus end organization and Golgi morphology. *J Cell Biol* 216:3179-98.
- Zan J, An ST, Mo KK, et al., 2016. Rabies virus inactivates cofilin to facilitate viral budding and release. *Biochem Biophys Res Commun* 477:1045-50.
- Zan J, Liu S, Sun DN, et al., 2017. Rabies Virus Infection Induces Microtubule Depolymerization to Facilitate Viral RNA Synthesis by Upregulating HDAC6. *Front Cell Infect Microbiol* 7:146.
- Zhang R, Alushin GM, Brown A, et al., 2015. Mechanistic Origin of Microtubule Dynamic Instability and Its Modulation by EB Proteins. *Cell* 162:849-59.
- Zhang R, Liu C, Cao Y, et al., 2017. Rabies viruses leader RNA interacts with host Hsc70 and inhibits virus replication. *Oncotarget* 8:43822-37.